

C3 Survey of Solar System Asteroids

Glenn E. Peterson* and Alisa M. Hawkins†
The Aerospace Corporation, El Segundo, CA, 90254

A trajectory analysis survey of Potentially Hazardous Asteroids (PHAs), which are defined as any asteroid whose current orbit approaches the Earth’s orbit to within 0.05 AU, was conducted. The goal of the survey was to determine the percentage of PHAs that could be reached by a spacecraft originating from the Earth as a function of the energy required, which is proportional to C3. The results of the study found that the C3 requirements were reasonable only in cases where time permitted favorable geometries between the Earth and the PHA. In all other cases that imposed launch and arrival time constraints, such as in a crisis situation, the C3 requirements were increasingly restrictive and only a small percentage of the PHA population was within expected launch/mission capabilities. In such cases, advanced warning of an impending threat is crucial in relaxing the mission time constraints and reducing the required C3 to feasible levels.

I. Introduction

Previous Potentially Hazardous Asteroid (PHA) trajectory studies¹⁻⁵ performed detailed mission analysis on a small number of catalog objects or reference missions, such as Apophis. In order to evaluate how effective mitigation scenarios are for an unforeseen threat, a more general analysis detailing mission requirements for trajectories reaching the entire PHA population was needed. The purpose of the current study is to characterize the PHA population in terms of the energy required to go from the Earth to the PHA. This was deemed a useful metric for missions that either characterize or mitigate PHAs.

For planetary missions, it is common to report the launch energy requirements of the mission in terms of C3 values. This term is derived from the energy equation, Eqn. 1, where ξ is defined as the specific mechanical energy, μ is the gravitational constant, r is the orbital radius, and v is the orbital velocity. In the hyperbolic case, as r goes to infinity, the energy equation is equivalent to the velocity squared divided by two, as in Eqn. 2. This velocity (v_∞), known as the “excess velocity,” is the velocity at which the spacecraft will depart the gravitational body. C3 is simply the square of the excess velocity,⁶ which is proportional to the energy required to depart Earth and enter onto a desired transfer orbit. Launch vehicle providers often give launch vehicle payload capabilities as a function of C3, because this value is independent of the parking orbit used. In order to avoid confusion, the term C3 is typically used when departing a celestial object (*e.g.*, leaving Earth) and the term v_∞ is used when approaching a celestial object (*e.g.*, arriving at the PHA). Because the PHA has very small mass, the v_∞ can be thought of as either the deltaV needed to match the velocity of the PHA (as with a rendezvous mission) or the speed at which the vehicle will flyby the PHA. In this document, the terms v_∞ and arrival speed are used interchangeably.

$$\xi = \frac{v^2}{2} - \frac{\mu}{r} \quad \text{Eqn. (1)}$$

$$\frac{v_\infty^2}{2} - \frac{\mu}{r_\infty} \Rightarrow \frac{v_\infty^2}{2} = \frac{C_3}{2} \quad \text{Eqn. (2)}$$

* Manager, Astrodynamics Department, M4/946, and AIAA Member.

† Member of the Technical Staff, Astrodynamics Department, M4/948, and AIAA Member.

II. Asteroid & PHA Distributions

The first part of the analysis was to examine the orbit element distribution of the overall asteroid population and the smaller PHA population. There are almost 340,000 asteroids that have been cataloged within our solar system;⁷ of these 1183 were identified as being PHAs. The typical definition used to distinguish a PHA is that the orbit of the asteroid comes within 0.05 AU of the Earth's orbit⁸ (i.e., a mean orbit intersection distance (MOID) of less than 0.05 AU), and that its absolute magnitude is less than or equal to 22 (asteroid diameter greater than approximately 140 meters). For ease of computation, a slightly more conservative orbit definition

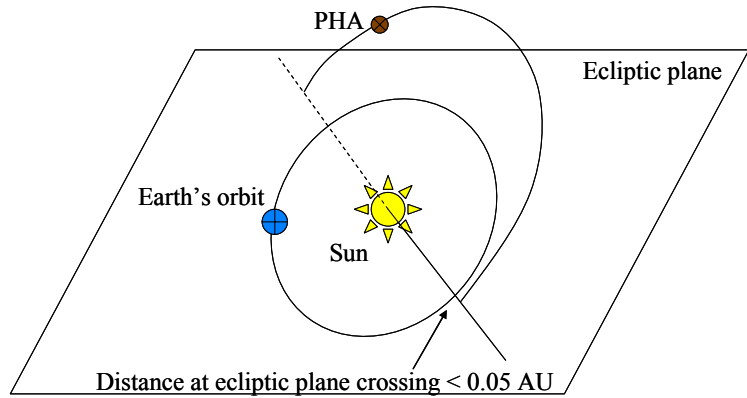


Figure 1. PHA definition.

was adopted for this study consisting of computing the PHA's distance from the Sun when the PHA intersected the plane of the ecliptic (equivalent to Earth's orbit plane; Figure 1). When this distance was less than 0.05 AU from any part of the Earth's orbit, that object was identified as a PHA. Since the Earth's orbit has an eccentricity of ~ 0.0167 , this amounted to a definition for a PHA as any object with nodal distance between 0.9333 AU and 1.0667 AU. This definition results in a slightly higher number of PHAs than identified through a MOID of less than 0.05 AU. For example, the JPL Near-Earth Object website lists 804 objects as PHAs.⁸ These two groups, all asteroids and those defined as PHAs, formed the basis of the available objects used for this study. It should also be noted that of the 1183 PHAs, there were 64 objects identified as being both ascending and descending node crossers.

There is also the issue of asteroid taxonomy, which is not fully addressed in this document, but is important when considering mitigation and characterization missions. Depending upon the classification scheme, there may be up to 19 different physical types of asteroids. The dominant types are: the carbonaceous (C-type, anywhere from ~ 42 -75% depending upon the classification system), siliceous (S-type, ~ 17 -27%), and metallic (M-type, ~ 10 %). Since the type of mitigation mission that would be mounted may be heavily influenced by the type of PHA to be moved, the physical characteristics of the PHA are important design parameters. However, it is much easier to determine an asteroid's orbit than its taxonomy, and few PHAs have had their taxonomy clarified to a high level of confidence. In essence, while the orbits of asteroids and PHAs are well known, their physical classification is not.

Figures 2-6 depict the distribution of asteroid and PHA orbit elements for the semi-major axis, eccentricity, inclination, argument of perihelion, and right ascension of ascending node, respectively. The y-axis of each of these plots is the percentage of the entire population in a particular bin. Note that since the asteroid population has about 340,000 objects and there are only 1183 PHAs, the same percentage value represents a different number of actual objects for the two populations.

The inclination, argument of perihelion, and right ascension of ascending node are similar in their distributions for the two groups. The inclination plot in Figure 4 shows that most asteroids and PHAs have relatively low

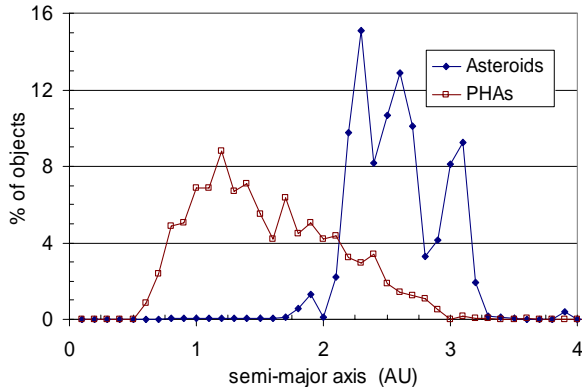


Figure 2. Semi-major axis distribution of asteroids.

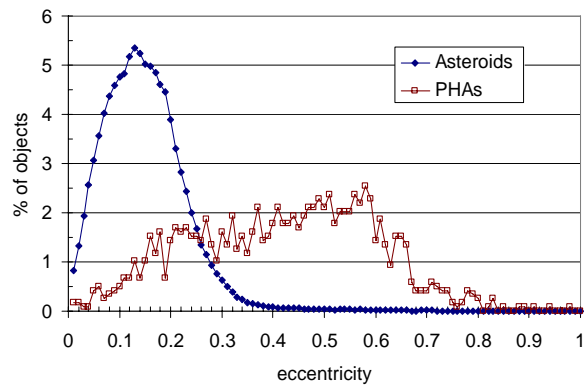


Figure 3. Eccentricity distribution of asteroids.

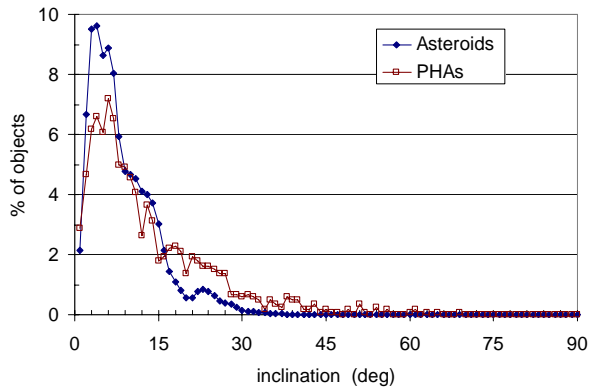


Figure 4. Inclination distribution of asteroids.

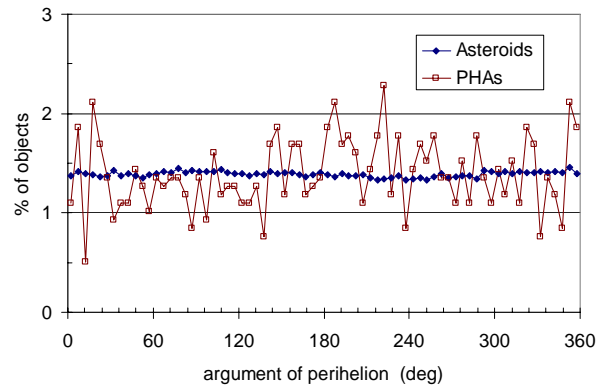


Figure 5. Argument of perihelion distribution of asteroids.

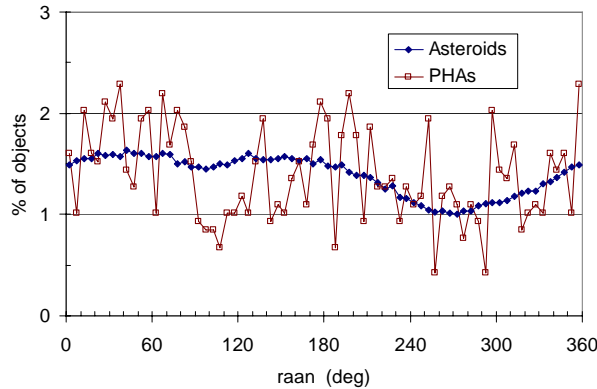


Figure 6. RAAN distribution of asteroids.

inclinations of less than 30 degrees with respect to the ecliptic plane. However, it should be noted that for purposes of mission planning nearly all potential missions to a PHA must take into account the difference between the orbital planes of the Earth and the PHA. In short, for every degree change in spacecraft's orbit plane (i.e., going from the Earth to the PHA), approximately 500 m/s deltaV must be applied. Only missions that intercept the PHA as it crosses the ecliptic plane may be able to avoid these additional costs; however, the ecliptic-crossing intercept missions have limited applications when trying to accurately characterize or mitigate a PHA. To heighten the scientific return or increase the deflection capability, it will be necessary in most cases to rendezvous with the PHA of interest out of the ecliptic plane. In Figures 5 and 6, the argument of perihelion and right ascension of ascending node both show fairly even distributions; however, there is some slight variation in the right ascension. Looking at the asteroid population RAAN curve in Figure 6, there is a dip seen near RAAN values of 270 deg. This RAAN region, where a smaller percentage of asteroids lie, probably has a dynamical significance (e.g., disturbances by Jupiter, solar radiation pressure, etc.), and should be a topic of further research. The PHA RAAN curve in this same figure does not show as noticeable trends, but this may be due to the small sample size.

While the angular arguments are similar between the two populations, the semi-major axis and eccentricity are not. This is not unexpected since most asteroids are located in the asteroid belt and hence are fairly circular, while most PHAs have a smaller semi-major axis and are more elliptical (by necessity since they must cross the Earth's orbit.) Similar to the inclination effect, the higher eccentricities imply that rendezvousing with PHAs requires substantial deltaV (~1.5 km/s for every 0.1 change in eccentricity).

Figure 7 shows the nodal distance distribution for both the ascending and descending nodes for the asteroid population (i.e., total number of ecliptic crossings is equal to twice the total number of objects.) The asteroid belt and the PHA region are explicitly marked. The asteroid distribution spike at Earth distance should not be taken as an indication of a greater concentration of objects at Earth distance, but rather is an artifact of Earth observers seeing more of these objects as they pass close by the Earth. This is further supported by Figure 8, which shows the

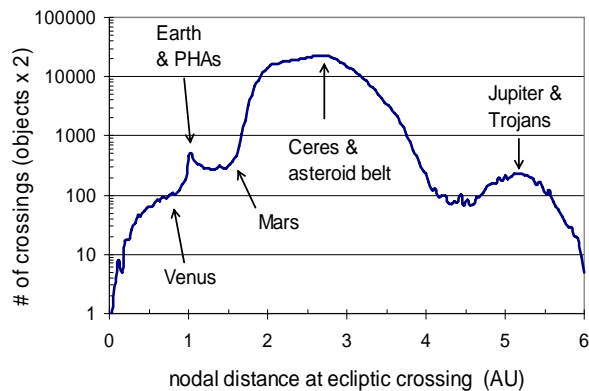


Figure 7. Nodal distance distribution of asteroids.

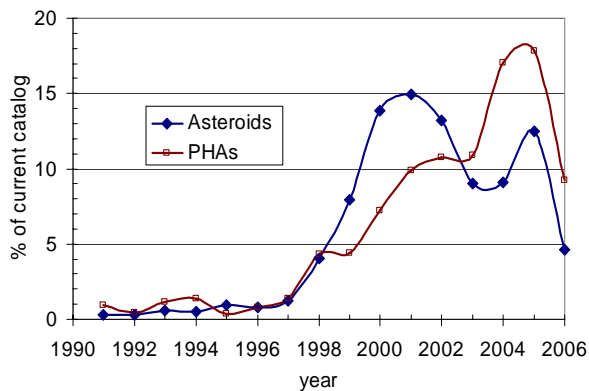


Figure 8. Asteroid & PHA discovery dates by year.

discovery dates for the asteroid population, as well as those objects identified in this report as PHAs. The trends suggest that there has been a switch in the last few years to discover and identify PHAs, as opposed to the overall asteroid population. This contributes to the spike seen in Figure 7. However, the dip in Figure 7 just beyond Earth's orbit implies that there may be many asteroids between Mars and Earth that have not been identified.

III. C3 Requirements

The second part of the study was to determine the minimum launch C3 that would be required for a spacecraft to go from Earth to the PHA. The C3 computation was performed for three scenarios (Figure 9). The first was to set the launch date and allow the asteroid to vary in its orbit. This might represent a mission scenario where the spacecraft had to leave the Earth by a fixed date due to launch pad/budget/manufacturing/political conditions, but as long as it reached the PHA, the mission could be accomplished. The second scenario consisted of fixing the arrival date at the asteroid and letting the Earth launch date vary. This would represent a mitigation mission where the launch date was not constrained, but the spacecraft had to get to the asteroid by a fixed date in order to impart the necessary change to the PHA's orbit to prevent impact. The third scenario was to let both the launch date and the arrival date vary. This might represent a precursor mission that would characterize a PHA well in advance of its projected time of closest approach with the Earth. For this type of precursor mission, there would be more flexibility in the launch and arrival dates and the mission could wait until the most favorable relative geometry was achieved.

For each of the three scenarios, the minimum launch C3 was computed for three conditions: the C3 required to launch the spacecraft onto an intercept course with the PHA without regard to the arrival conditions, rendezvous with the PHA (minimization of the sum of the launch and arrival speed C3s), and minimization of just the arrival speed without concern for the launch C3. Since the goal was to produce a statistical summary of the C3 requirements, the minimum C3 for each PHA was found over the search space, and a cumulative histogram was generated that would show what percentage of the PHA population could be reached for each of the scenarios as a function of C3.

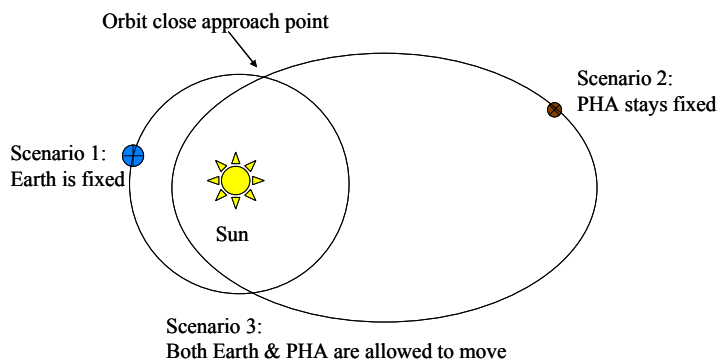


Figure 9. Geometry of different scenarios.

A. Scenario 1: Fixed Launch Date

In the first scenario, the Earth was set to be at a fixed point in its orbit (i.e., fixed launch date). The asteroid was allowed to propagate for a total of 5 years from the launch date with a Lambert solution computed at time steps of 1-day intervals. The launch C3 over the 5 years of propagation was saved separately for the three conditions. For example, consider that the spacecraft left Earth on January 1, 2010 and that Apophis was the target asteroid. Then Apophis would be propagated from January 2, 2010 to January 1, 2015 at one-day intervals. At each day of the Apophis propagation, a Lambert solution would be computed. That is, while the Earth remains fixed, the time of flight to Apophis changes for each solution. The results of the Apophis case are shown in Figure 10 for the launch-to-intercept condition. The spikes in the plot reflect the times when the Lambert solution switched from going the long way around the transfer orbit to Apophis to the short way and vice versa. For each PHA, a curve such as Figure 10 would be produced and the minimum launch C3 would be saved. The launch C3 for the minimum rendezvous case and the launch C3 for the minimum arrival speed at Apophis would be similarly computed. The launch-to-intercept, rendezvous, and minimum arrival speed C3s would not necessarily be the same, as different transfer trajectories could produce different optimal launch C3s. Each of the 1183 PHAs was examined in this manner, and the percentage of PHAs reachable for a given C3 was computed.

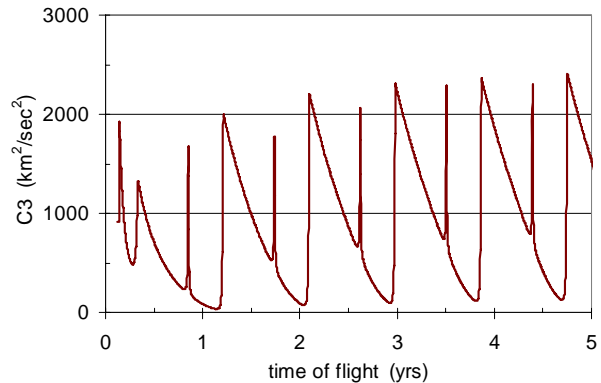


Figure 10. Required launch C3 for Apophis and a launch date of 1-1-2010.

The results of this analysis are shown in Figures 11 and 12 for a launch date of January 1, 2010. Figure 11 shows the percentage of the PHAs reachable for a given launch C3. The C3 values are rather high. For example, the Aries CALV, with a payload of 38000 kg, could supply a C3 of 25 km²/sec² implying that such a vehicle could only intercept about 40% of the PHAs should launch date be a constraint on the mission (i.e., a crisis situation). For rendezvous, it would be even lower at 27% and to get to the lowest possible arrival speed (a desirable state for a characterization mission), only ~8% of the PHAs are reachable for a C3 of 25 km²/sec².

Figure 12 shows the arrival speed corresponding to the solutions of Figure 11. As expected, the minimum arrival speed curve is the most optimal solution with rendezvous (minimizing the sum of the launch and arrival C3s) being the next most optimal and finally the launch-to-intercept case (minimizing the launch C3 without regards to its effect on the arrival speed). It is apparent that the arrival speeds for this case are also high, even for the minimum solution. Higher arrival speeds mean that a spacecraft either has to get the desired science from a fast flyby or a substantial amount of fuel must be carried on board to slow the vehicle down to the point where the science/mitigation requirements can be met.

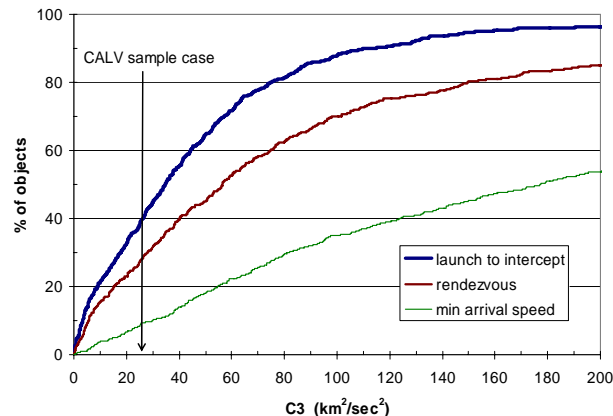


Figure 11. Launch C3 for fixed launch date of 1-1-2010.

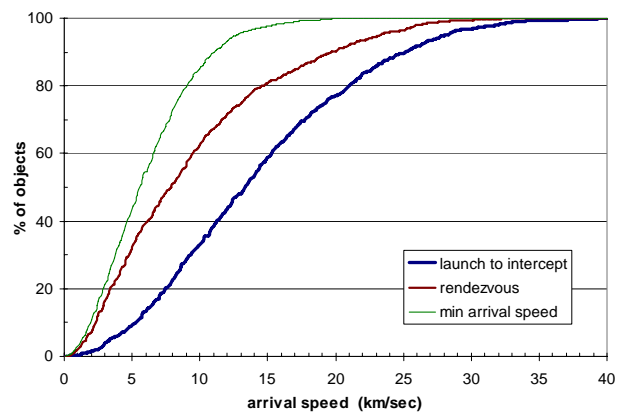


Figure 12. Arrival speed for fixed launch date of 1-1-2010.

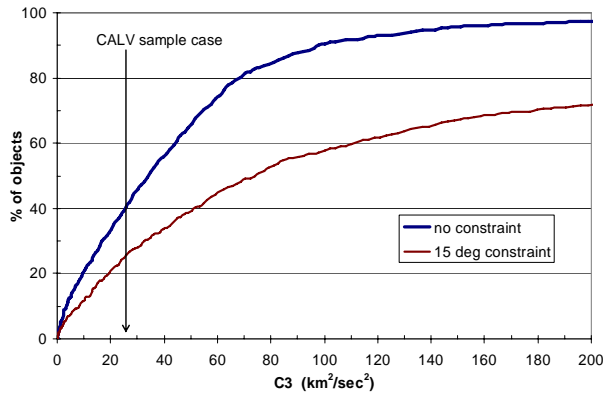


Figure 13. Available PHAs for the launch-to-intercept condition as a function of C3 for launch date of 1-1-2010.

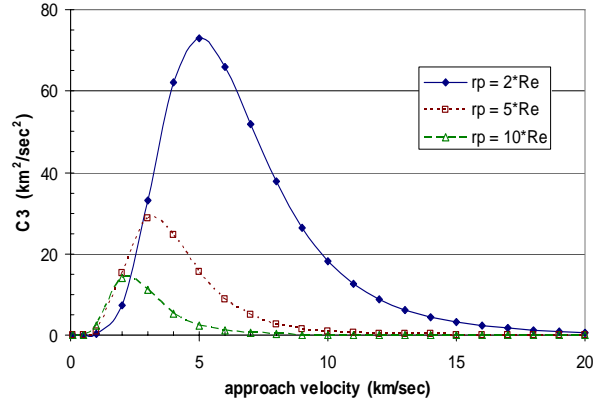


Figure 14. C3 requirement reduction from an Earth flyby for various perigee flyby distances

An additional solution was examined wherein an angular constraint was placed upon the approach angle to the PHA of 15 degrees. This constraint would represent the end-point requirement for a kinetic impactor that needed to either push or slow the PHA by directing its force as close as possible to the pre-existing velocity vector of the PHA. The constraint was added to the Lambert solver and the solutions recalculated, in which new solutions (*i.e.*, different arrival dates) were obtained for PHA cases that originally violated the constraint. Figure 13 shows the result for the launch-to-intercept condition with and without the angular constraint. For the CALV example given above, imposing a 15 degree angle constraint would reduce the PHAs that could be reached under this scenario from ~40% to ~25%. For the rendezvous and minimum arrival speed cases, the percentage of reachable PHAs would drop from 27% to 18% and from 8% to 1% (not shown in Figure 13). If other constraints on the mission are added, such as line-of-sight communications between the spacecraft and the Earth during mission critical events, the impact on the C3 requirements would be even more pronounced.

Part of the difficulty in achieving the high C3 values depicted in Figures 11 and 13 can be somewhat mitigated through single or multiple planetary flybys. In a planetary flyby, the direction of the spacecraft's planet-relative velocity is altered by the gravitational pull of the planet which it is passing. This results in an apparent heliocentric velocity change of the spacecraft, and changes the spacecraft's heliocentric trajectory. For a notional analysis, it is simplistically assumed that the ΔV change due to the flyby can be directly subtracted from the departure velocity required to leave Earth. This value is squared to get an estimate of how much the required C3 would change. Figure 14 shows the results of this notional analysis for an Earth flyby, giving an idea of how the C3 requirements can be reduced by performing an Earth flyby. This is plotted for various minimum miss distances between the flyby orbit and the Earth, where R_e is the Earth radius (6378.137 km) and r_p is the perigee radius. The closer in to the Earth the spacecraft comes during its flyby, the more boost it will obtain, and the less C3 will be required at launch. However, if the spacecraft is carrying a politically sensitive payload or if time of flight is a consideration, then a close flyby, or for that matter any flyby at all, may not be feasible.

B. Scenario 2: Fixed Arrival Date

In the second scenario, the launch date was varied over a 5 year time span and the PHA arrival date was fixed. This approach represents a scenario where the mission has a flexible launch date, but the arrival date is critical. One example is a mitigation mission that must rendezvous with a PHA while not in close proximity of Earth. For this study, the initial position of Earth was varied from January 1, 2010 to November 15, 2014, in one-day increments. The PHA arrival date was fixed at January 1, 2015. For each launch date, a Lambert solution was found between Earth and the PHA at the arrival time. Again, the minimum solutions for intercept, rendezvous, and minimum arrival speed were recorded separately. Keep in mind that Lambert solutions do not take into account possible $\Delta V/C3$ cost savings through planet gravity assists or low thrust trajectories.

The fixed arrival time results are displayed in Figures 15 and 16. The first v_∞ of the Lambert solution is converted to a Launch C3 for launch vehicle sizing. Fixing the arrival time results in similar statistics to fixing the launch date; however, the required C3 values are seen to be slightly higher. This varied only slightly when this same analysis was performed for different arrival dates. As seen in Figure 15, the launch-to-intercept trajectories require the lowest C3 values to reach the greatest percentage of the PHA population, while minimizing the arrival speed

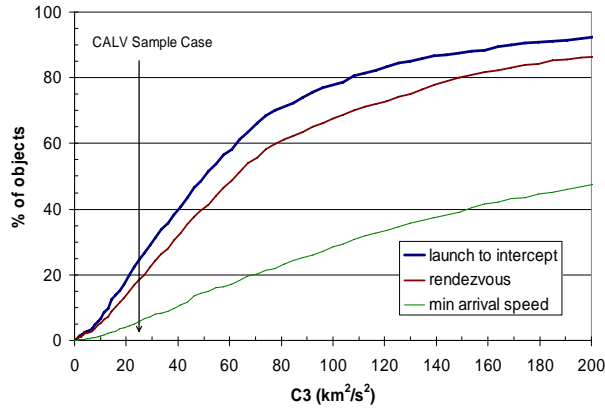


Figure 15. Launch C3 for cases with fixed PHA arrival time.

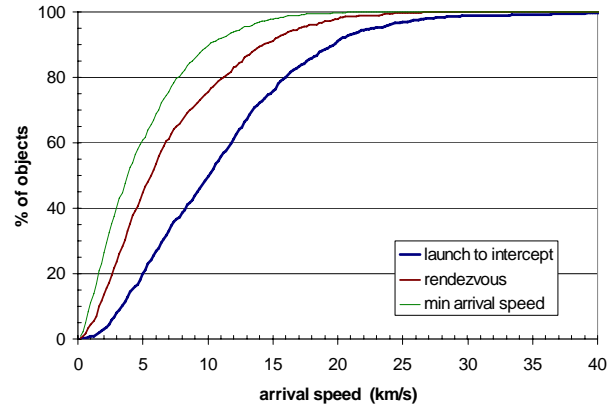


Figure 16. Arrival speed for cases with fixed PHA arrival time.

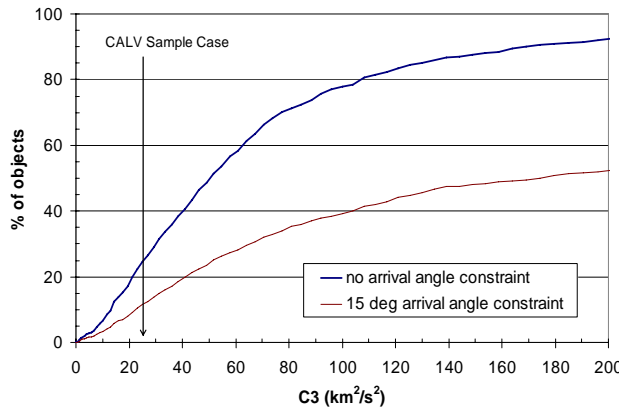


Figure 17. Arrival Angle Constraint Comparison for Intercept Trajectories.

causes the launch C3 requirements to increase. The rendezvous curve is a compromise between the launch C3 and arrival speed.

The arrival speeds of the intercept missions are seen in Figure 16 to be as much as 20 km/s. At this high of an intercept speed, it may be difficult to gain useful information of the PHA characteristics for a characterization mission, and therefore some additional energy may be required to slow the intercept speed. The rendezvous curve represents a balance between C3 and arrival speed and does not exhibit as high arrival velocities as the launch-to-intercept case. The thin green line shows the lowest possible arrival speed that would be required on-board the vehicle to rendezvous. For a fixed arrival time, a minimum of 10 km/s will be needed on-board the vehicle to rendezvous with 90% of the PHA population.

For some mitigation missions, it is advantageous to approach the PHA from either a head-on or tail-end direction, instead of from the side. This is especially true for an impact technique, as this increases the momentum transfer from the impactor to the PHA. A constraint was added to the Lambert solution to see how a 15 degree arrival approach angle limitation would alter the results. As seen in Figure 17, the launch C3 increases significantly when this constraint is imposed. Given a launch C3 of 25 km²/sec² and an intercept mission that required a fixed arrival time, 25% of the PHA population can be reached if there is no arrival angle constraint, as opposed to 12% when the constraint is imposed.

C. Scenario 3: Varying Launch and Arrival Date

The third scenario consisted of letting both the launch and arrival date vary. This was done by varying the launch date in 1-day increments for 5 years, and letting the arrival date vary between 1 day and 5 years from the specified launch date. Therefore, in each run the possible time-of-flight ranged from 1 day to 5 years. This scenario is again representative of a mission where the specific launch or arrival dates do not matter; instead, simply getting to the PHA is sufficient to accomplish the mission goals. Figure 18 shows the reason why varying both the launch date and arrival date are important for finding the true minimum C3. Two sample PHAs are depicted with the C3 required to

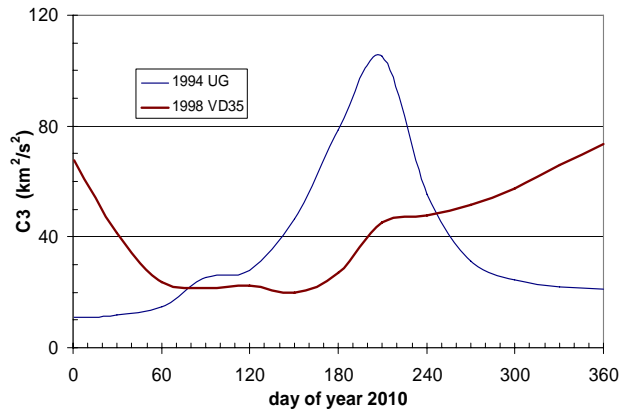


Figure 18. Launch C3 temporal variation for two sample PHAs.

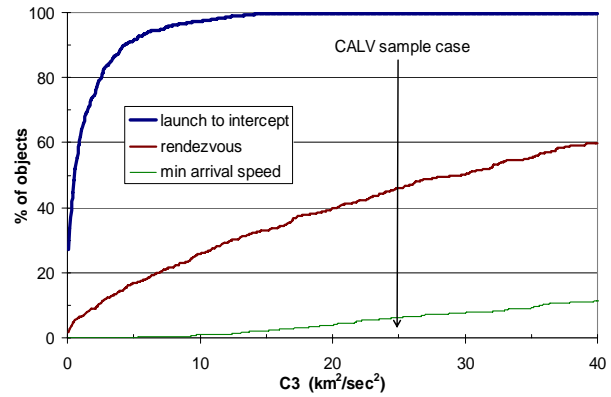


Figure 19. Launch C3 when both launch and arrival date vary.

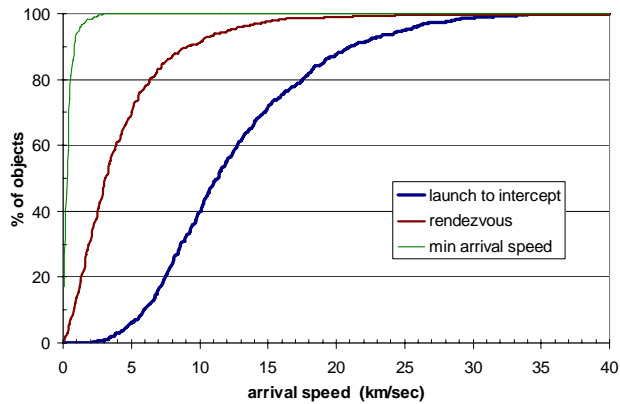


Figure 20. Arrival speed when both launch and arrival date vary.

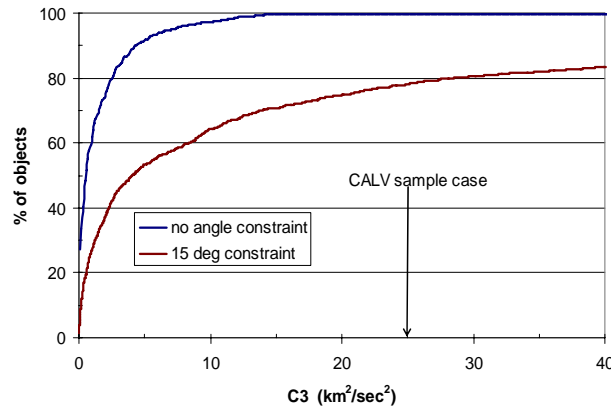


Figure 21. Required launch-to-intercept C3 for varying launch and arrival dates with angle constraint of 15 degrees.

intercept given as a function of launch date. If a launch date of January 1, 2010 is chosen, then a C3 of about 10 km^2/sec^2 is required to get to 1994 UG while the same PHA would require a launch C3 of over 100 km^2/sec^2 if the launch date was seven months later. Similarly, 1998 VD35 has a high C3 of about 70 km^2/sec^2 on January 1, 2010, but a C3 of 20 km^2/sec^2 just two months later. Therefore, if there are no mission constraints on the arrival time or the launch date, then a potentially much lower C3 may be necessary to reach a particular PHA than was otherwise found earlier.

Figure 19 shows the launch C3 statistical summary. Comparing this plot with Figures 11 & 15, the launch C3 requirements when both launch and arrival dates are allowed to vary are much lower than either of the two more restrictive cases. For the CALV sample case of a C3 of 25 km^2/sec^2 , all but two of the PHAs are reachable for a direct intercept without regards to arrival conditions. Geometrically, this represents a situation where the arrival date occurs when the PHA crosses the plane of the ecliptic. The rendezvous and minimum arrival speeds are similar to each other with 45% of the PHAs reachable for a C3 of 25 km^2/sec^2 for rendezvous and 40% for minimum arrival speed.

Figure 20 shows the corresponding arrival speed for the solutions of Figure 19. Comparing this plot with Figures 12 & 16, the launch-to-intercept case for the three scenarios is very similar in terms of arrival speed, but the rendezvous and minimum arrival speeds provide a noticeably better solution when both parameters are allowed to vary. Figure 21 shows the launch-to-intercept case when the 15 degree approach angle constraint is added. As with the earlier scenarios, adding the constraint inhibits the number of PHAs that can be reached for a given C3. For the fixed launch date scenario (Figure 14), the percentage dropped from 40% to 25%, and in the fixed arrival date scenario (Figure 18), it dropped from 28% to 13%. The results in Figure 22 for this scenario indicate the percentage decreased 100% (all but two PHAs) to 78%.

D. Hohmann Transfer Analysis

Analysis using a Hohmann transfer was performed to add validity to the results. A Hohmann transfer represents the minimum energy transfer between two orbits and does not take into account phasing between the two objects. Results obtained from a Lambert solution should require more C3 and/or deltaV than a Hohmann solution. For this Hohmann transfer analysis, the Earth is assumed to be in a circular orbit with a radius of 1.0 AU. Earth and the PHAs will first be assumed to reside in the same plane, and then a plane change maneuver will be included in the results. In performing a Hohmann transfer from a circular orbit to an elliptical orbit, there are two options available: 1) target apohelion of the elliptical orbit, then change perihelion, 2) target perihelion of the elliptical orbit, then change apohelion. These two transfers are illustrated in Figure 22. The total impulsive deltaV (ΔV_T) is the summation of the two individual impulsive burns (ΔV_1 and ΔV_2).

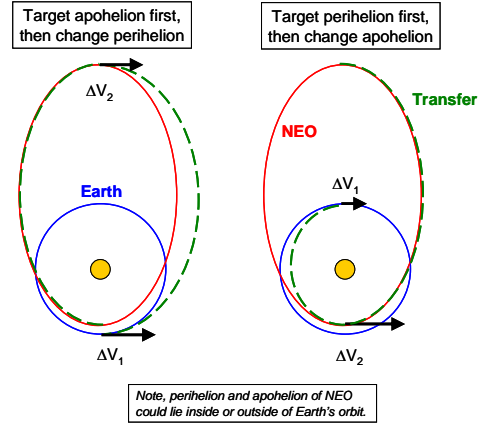


Figure 22. Hohmann transfer options between circular and elliptical orbits.

Hohmann solutions were obtained from Earth to each of the objects in the PHA population, using both types of transfers above.

Similarities between these Hohmann results and the Lambert solutions are drawn. In the case where only an intercept of the PHA is desired, the solution having the minimum ΔV_1 was recorded, which is analogous to the previous launch-to-intercept cases. In most cases, this solution consisted of the second type of Hohmann transfer because the PHA perihelion is usually closer to the Earth's orbit than the PHA apohelion, requiring less orbital adjustment. To compare the Hohmann solutions to the Lambert rendezvous cases, the minimum ΔV_T was recorded. Lastly, to compare to the minimum arrival speed cases, the Hohmann transfer that required the minimum ΔV_2 was recorded. The rendezvous and minimum arrival cases consisted mainly of the first type of Hohmann transfer, as this transfer typically requires less ΔV_T and has a slower arrival speed.

The Hohmann results where Earth and the PHAs are assumed to reside in the same plane are illustrated in Figure 23. This would represent an ecliptic-crossing intercept, where the vehicle stays in the same plane as Earth and intercepts a PHA as it passes through the ecliptic plane. These C3 values are similar to those seen when allowing both the launch date and arrival date to vary in the previous analysis. By not requiring an inclination change, the energy expenditure is greatly reduced.

Solutions that do include an inclination change to match the PHA orbit are shown in Figure 24. For simplicity, it is assumed that the inclination change occurs at launch or is provided by the launch vehicle. It is therefore included in the launch C3; the inclination change impulsive deltaV (ΔV_{inc}) is added to the initial burn ($\Delta V_1 + \Delta V_{inc}$), and then the magnitude of the resultant vector is squared to obtain the C3. This assumption is not optimal, as the inclination change is typically split between the launch and arrival burns, but it is a good first order approximation. Including an inclination change drastically limits the percentage of the PHA population that can be reached with a given launch

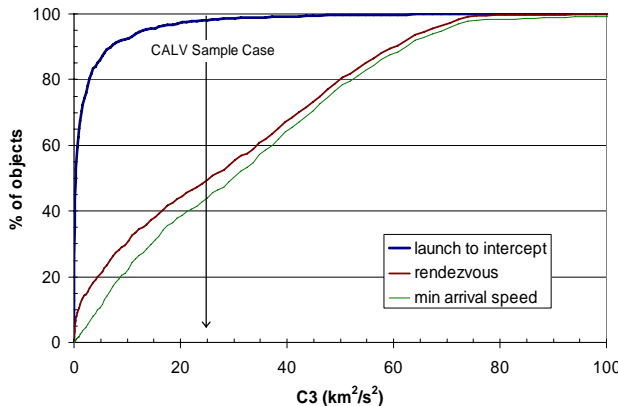


Figure 23. Hohmann transfer results without inclination change.

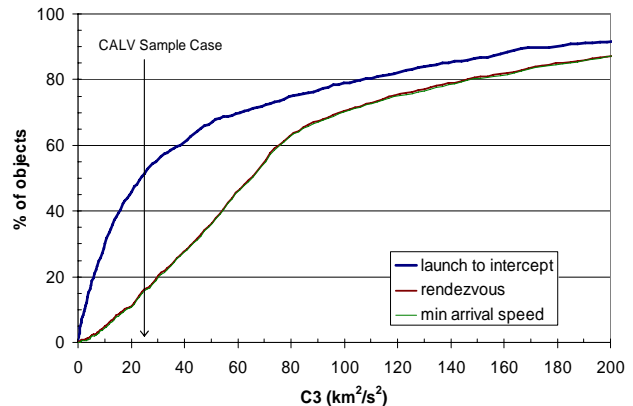


Figure 24. Hohmann transfer results with inclination change included in Launch C3.

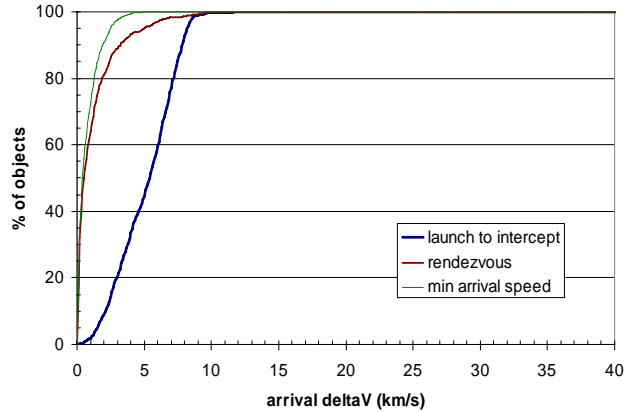


Figure 25. Hohmann transfer arrival deltaV.

C3. For example, the population of objects that can be intercepted with a C3 of 25 km/s is now only 52%, as compared to 98% with the simple planar Hohmann transfer solution.

The arrival impulsive deltaV (ΔV_2) for the Hohmann transfer solutions is illustrated in Figure 25. For this simplified analysis, ΔV_2 does not change based on the addition of an inclination change at launch. The solutions obtained here are closer to the analysis that varied both the launch and arrival date, again showing these results are closer to the optimal solution.

IV. Conclusion

The C3 requirements were found to be large for a mitigation mission in a crisis situation where the world cannot wait for a favorable relative geometry between the Earth and the PHA. This implies that advance warning of an impending impact is desirable from a mitigation perspective. For general PHA characterization missions, where there is no time pressure to evaluate or alter an impending threat, the C3 values are lower and within current and expected launch/mission capabilities. For in-between missions, such as characterization of a PHA that looks to be posing a threat, the C3 will also be between the worst and most favorable cases and will depend upon the individual PHA and its orbital geometry with respect to the Earth.

References

- ¹Adams, R.B., et al., "Survey of Technologies Relevant to Defense from Near-Earth Objects," NASA/TP-2004-213089, NASA Marshall Space Flight Center, Alabama, July 2004.
- ²Barrera, M. J., "Conceptual Design of an Asteroid Interceptor for a Nuclear Deflection Mission," *2004 Planetary Defense Conference: Protecting Earth from Asteroids*, Orange County, California, February, 2004.
- ³Bodnar, J., Cardenes, L., Hensley, J., Pitchford, B., Smith, T., "Near Earth Object Deflection Systems," *NASA Workshop on Near-Earth Object Detection, Characterization, and Threat Mitigation*, Vail Colorado, June 26-29, 2006.
- ⁴Smith, P.L., M. J. Barrera, E. T. Campbell, K. A. Feldman, G. E. Peterson, G. N. Smit, "Systems Design for Nuclear Deflection of a Near Earth Object Using Today's Space Technology," *2004 Planetary Defense Conference: Protecting Earth from Asteroids*, Orange County, California, February, 2004.
- ⁵Wie, B., "Solar Sailing Kinetic Energy Impactor (KEI) Mission Concept for Impacting and Deflecting Near-Earth Asteroids," *NASA Workshop on Near-Earth Object Detection, Characterization, and Threat Mitigation*, Vail Colorado, June 26-29, 2006.
- ⁶Moulton, F.R., *An Introduction to Celestial Mechanics: Second Revised Edition*, The Macmillan Company, New York, 1960.
- ⁷Lowell Observatory, Asteroid Observing Services, <http://asteroid.lowell.edu>, 2006.
- ⁸Jet Propulsion Laboratory, Near Earth Object Program, <http://neo.jpl.nasa.gov>, 2006.
- ⁹Bates, R. R., D. D. Mueller, J. E. White, *Fundamentals of Astrodynamics*, Dover Publications, New York, 1971.